

Report on Winter2014 Production: Image Differencing

March 6, 2014

Summary

Contents

1 Production Scope and Goals	3
1.1 Subtask 1: Reproduce W13 Results Using Current PhoSim	3
1.2 Subtask 2: Simulate Starfield using Multiple SEDs at a Single Airmass	3
1.3 Subtask 3: Simulate Starfield using Multiple SEDs at Multiple Airmasses	3
1.4 Subtask 4: Include Realistic Mix of Stars and Galaxies	3
2 Review of Wavelength Dependent Refraction	3
3 Running PhoSim	3
4 Analysis of Subtask 1	3
5 Analysis of Subtask 2	3
6 Analysis of Subtask 3	3
Appendices	16

1 Production Scope and Goals

- 1.1 Subtask 1: Reproduce W13 Results Using Current PhoSim**
- 1.2 Subtask 2: Simulate Starfield using Multiple SEDs at a Single Airmass**
- 1.3 Subtask 3: Simulate Starfield using Multiple SEDs at Multiple Airmasses**
- 1.4 Subtask 4: Include Realistic Mix of Stars and Galaxies**

Pushed back to S14.

2 Review of Wavelength Dependent Refraction

3 Running PhoSim

4 Analysis of Subtask 1

5 Analysis of Subtask 2

6 Analysis of Subtask 3

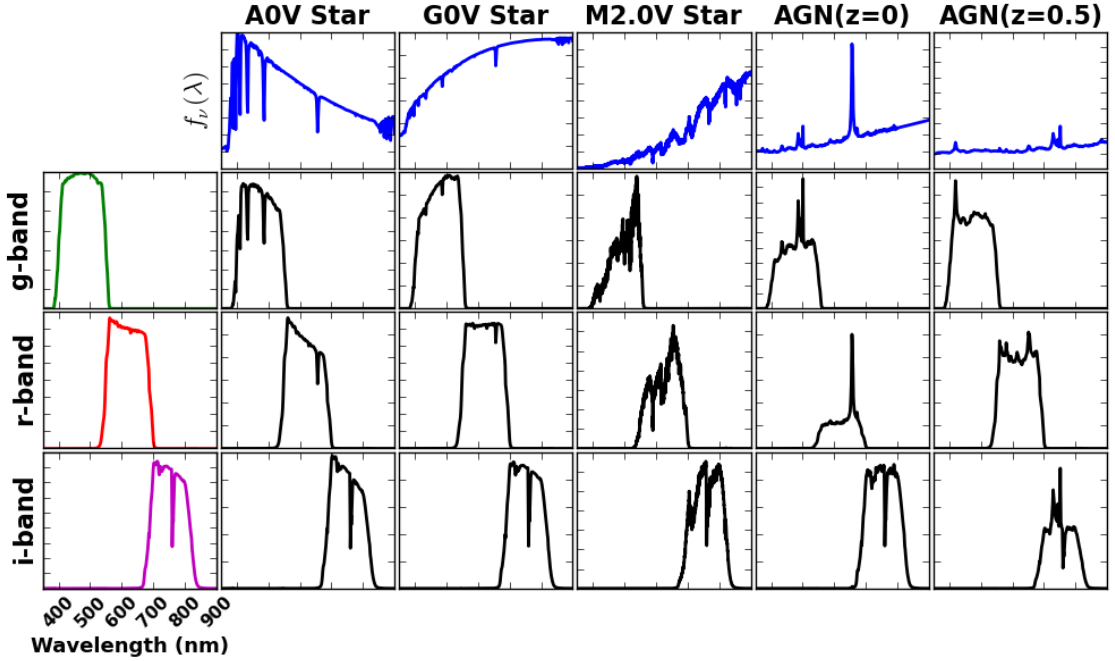


Figure 1: Effective Spectral Energy Distributions : The effective spectra of 5 reference objects – a “blue” A0V, a reference G0V, and a “red” M2.0V star, along with a QSO at redshift $z = 0$ and $z = 0.5$ – filtered through 3 transmission profiles corresponding to the LSST g , r , and i -bands. The top row shows the input spectral energy distribution $f_\nu(\lambda)$, while the leftmost column shows the LSST filter transmission profile in units of the normalized system response ϕ . The inner row/column figures show the effective spectrum of each SED (along columns) when multiplied through the respective filter (along rows). In all subpanels, the x-axis is wavelength. The A0V, G0V, and M2.0V spectra correspond to CAT_SHARE_DATA files `kp01_9750.fits_g45_9830.gz`, `km20_6000.fits_g30_6020.gz`, and `m2.0Full.dat.gz` respectively, and were used as the SEDs of the stars in the W14 image simulations. This figure may be recreated using the script `python/DCR.py`.

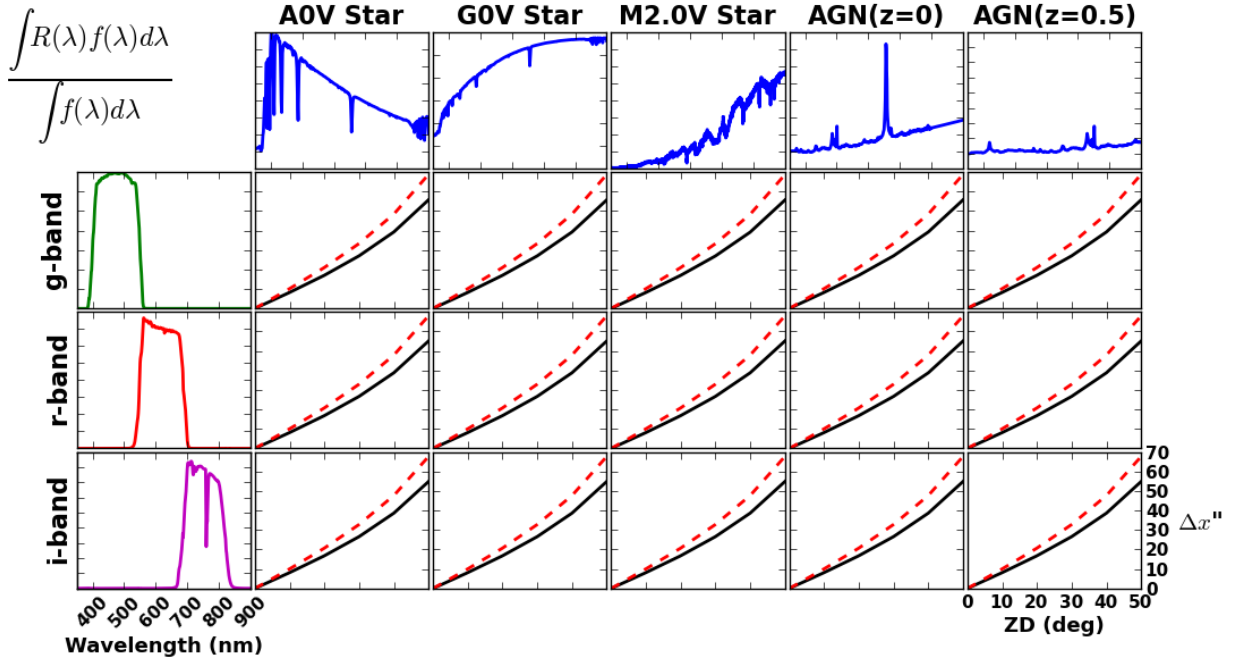


Figure 2: Refraction Amplitude vs. Filter and Spectral Energy Distribution: The flux-weighted amplitude of refraction (in arcseconds) for each of the filtered SEDs in Figure 1, as a function of zenith distance in degrees along the x-axis. The solid black line is the nominal result from Eqn ??, while the dashed red line ignores the corrections for temperature and pressure. Note the maximum amplitude of refraction reaches nearly 1 arcminute. This figure may be recreated using the script `python/DCR.py`.

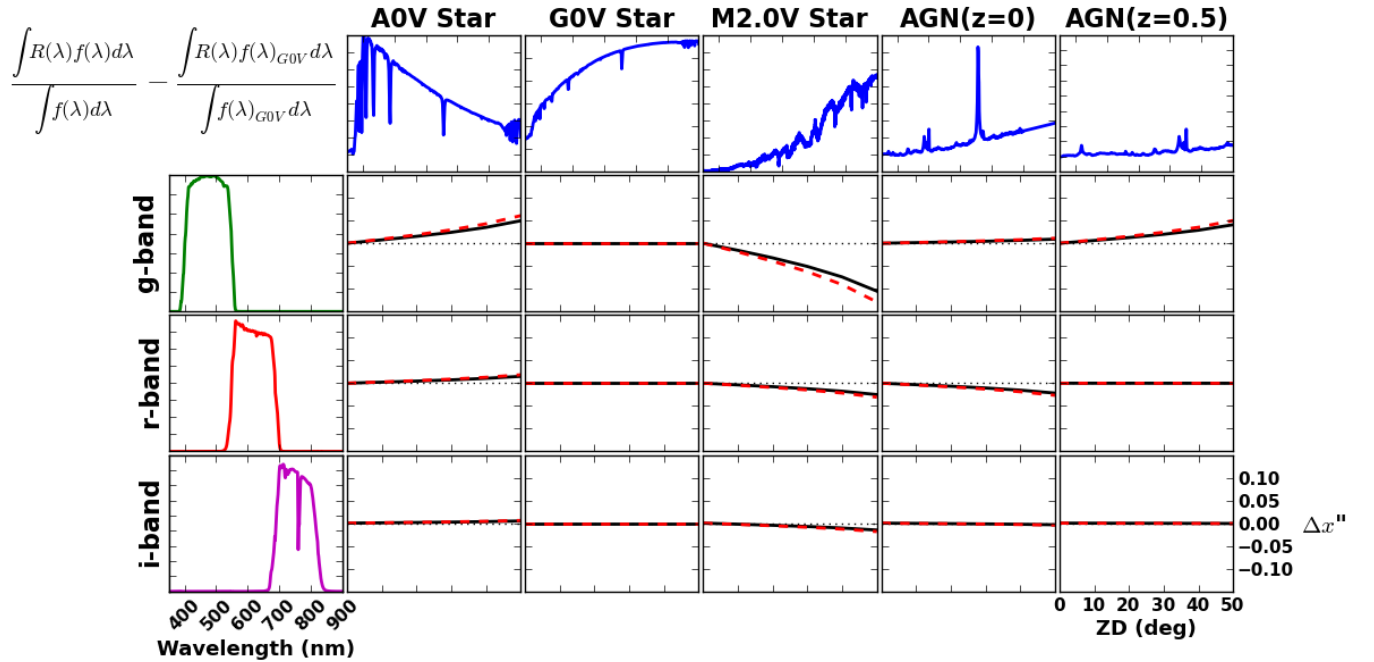


Figure 3: Differential Chromatic Refraction vs. Filter and Spectral Energy Distribution: The differential chromatic refraction of all sources from Figure 1 with respect to the reference G0V star, with respect to zenith distance. The maximum amplitude of DCR reaches $0.1''$, or approximately half an LSST pixel. This figure may be recreated using the script `python/DCR.py`.

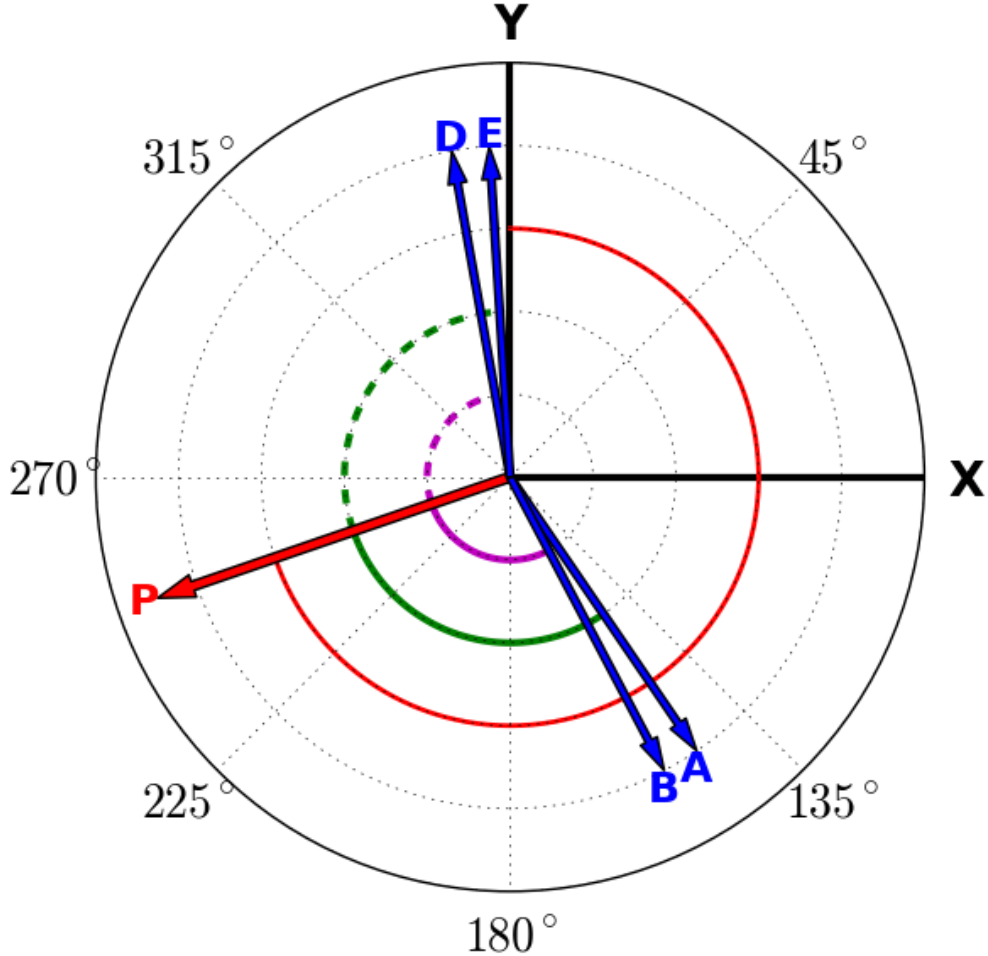


Figure 4: Designed Orientation of Dcr in W14 Phosim Runs: This figure represents the anticipated orientations of Dcr in the W14 phoSim data. The x,y coordinate system is depicted, as well as the convention that angles (`rotTelPos`, `rotSkyPos`) are clockwise with respect to the positive y-axis in the image coordinate system (counterclockwise in the camera coordinate system). The `rotTelPos` of 251 degrees specified for all simulations, which reflects the direction to the pole, is shown with the red vector Pand the red arc at $y=0.6$. The derived `rotSkyPos` for visits A,B,D,E are shown with the blue vectors, and reflect the angle towards zenith (the angle of increasing altitude). Dcr is expected to happen along these vectors. The angles PA,PE are similar, and represented by the green arcs; the angles PB,PD are also similar, and represented by the purple arcs. This is expected as observations A and E are taken at airmass 1.55 (zenith distance of 50 degrees) but at opposite sides of the meridian crossing of the star field; a similar situation was designed for observations B and D, which are taken at airmass 1.15 (zenith distance of 30 degrees). Visit C is not depicted as it was taken at zenith. This figure was created using the script `python/dcrSchematic.py`.

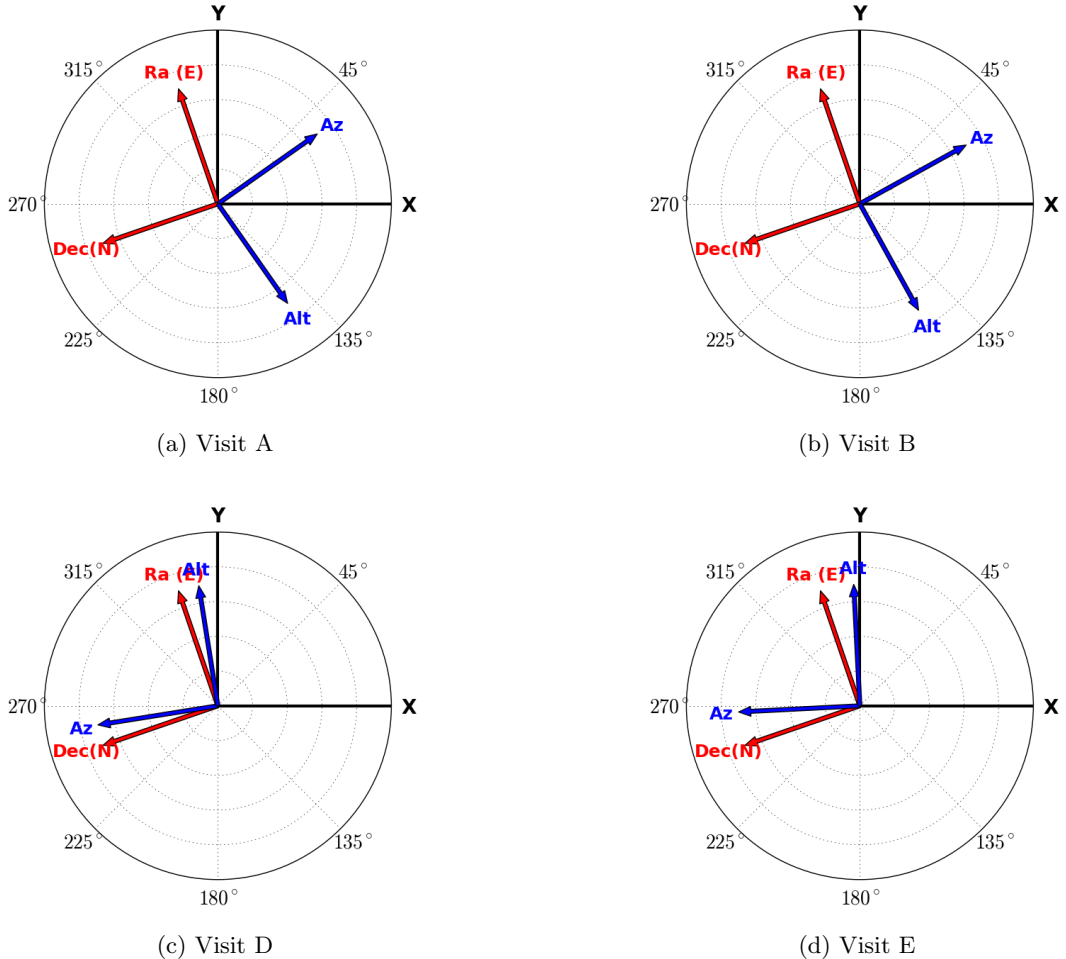


Figure 5: Wcs-Derived Orientations of Phosim Data: These figures show the orientations of the Right Ascension and Declination axes (red), and Altitude and Azimuth axes (blue) of visits A,B,D,E. Arrows represent the directions of *increasing* coordinate value. The Ra,Decl axes are the same in all images since they were designed to have a common `rotTelPos`. Ideally, the directions of increasing Alt will correspond to the `rotSkyPos` depicted in Figure 4. All coordinate system orientations were derived from the fitted Wcs of the `calexp` of the g -band observation of seeing values 2, i.e. the worst seeing image. To determine the orientations empirically, small steps were taken in each coordinate starting at the center of the image, and the Wcs and topocentric corrections used to map these back into offsets in the pixel plane. This figure was created using the script `python/compareDcrFromSims.py.py`.

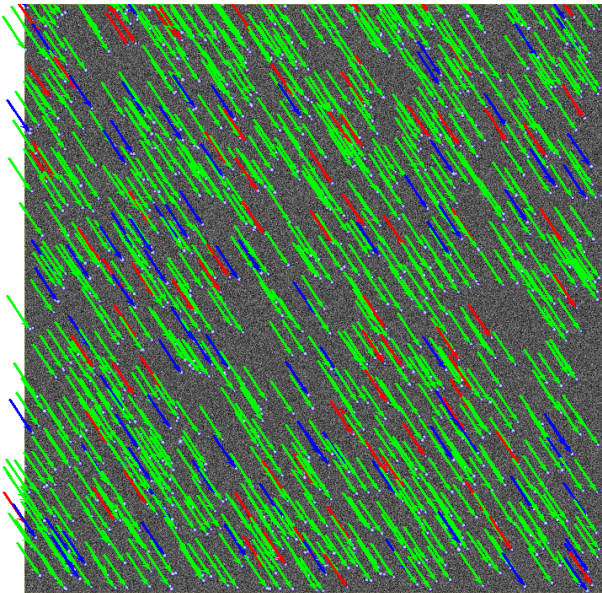


Figure 6: **Refraction:** This figure depicts the amplitude and orientation of the refraction vector in the visit A, `raft=2,2 sensor=1,1 filter=g`, seeing value 2 data. The vectors point from the unrefracted locations to the realized locations in the image. The SEDs of the sources are indicated with colors `blue`, `green` and `red` for AOV, GOV, and M2.0V respectively. This figure was created using the script `python/compareDcrFromSims.py`.

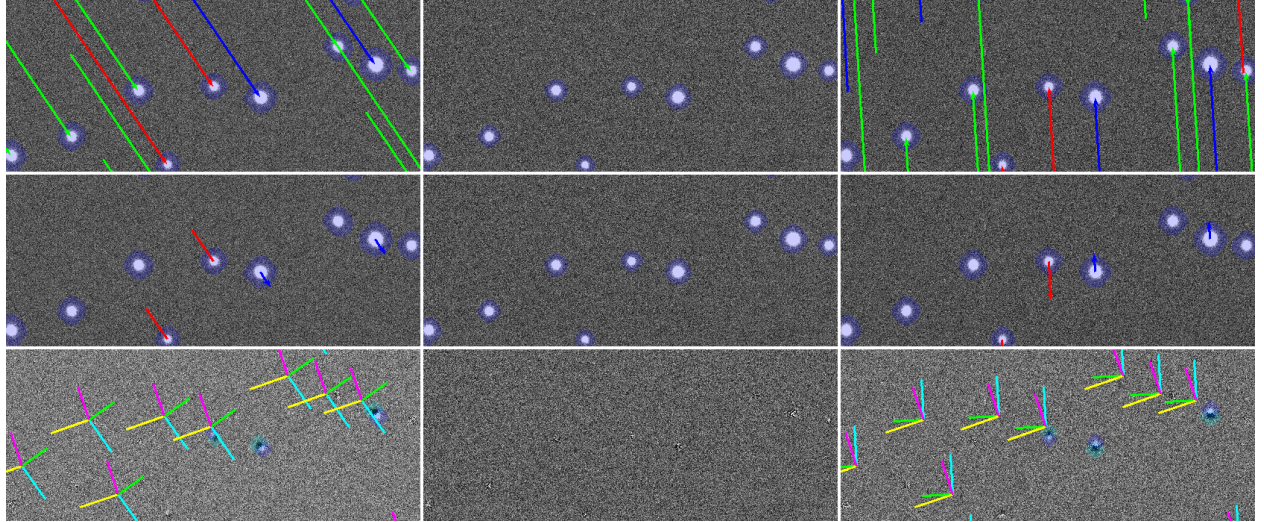


Figure 7: Differential Chromatic Refraction and Difference Image Quality, g -band: This set of panels demonstrates the amount of refraction (top row), differential refraction with respect to the GOV star (middle row), and the quality of the difference image (bottom row) for three sets of image differences. The first column uses science visit A, the middle C, and the third E. In all cases the template used was taken at zenith, i.e. visit C. The top rows effectively present the same information as Figure 6, but zoomed in on a particular cluster of stars. The second row subtracts off the green vector from all vectors. The residual refraction of the blue, red vectors represents differential chromatic refraction. These residual lengths have been multiplied by a factor of 100 for readability. Note that the blue vectors point along the vector to zenith, indicating the blue stars appear higher in the sky than their green counterparts, compared to an unrefracted observation. The red stars are not refracted as much and thus will appear lower in the sky. On the bottom row, we show the realized difference image quality. Note that the blue stars have positive lobes pointing along the direction to zenith, meaning the stars are “higher” in the sky w.r.t. the green stars when compared to the zenith template, while the dipoles of the red stars have the opposite polarity. For completeness, the Wcs-derived orientation of the Ra,Decl and Az,Alt coordinate axes are shown in the difference image (Ra,Decl,Az,Alt are magenta,yellow,green,cyan); see Figure 5 for more detail. This figure was created using the script `python/compareDcrFromSims.py`.

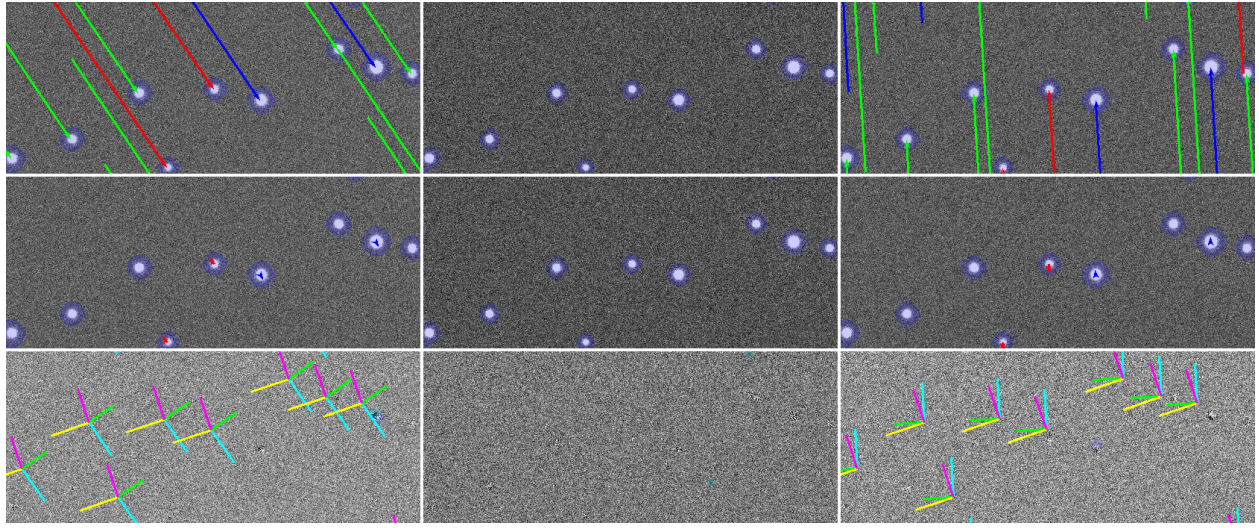


Figure 8: Differential Chromatic Refraction and Difference Image Quality, r -band: Same as Figure 7, but for r -band data. This figure was created using the script `python/compareDcrFromSims.py`.

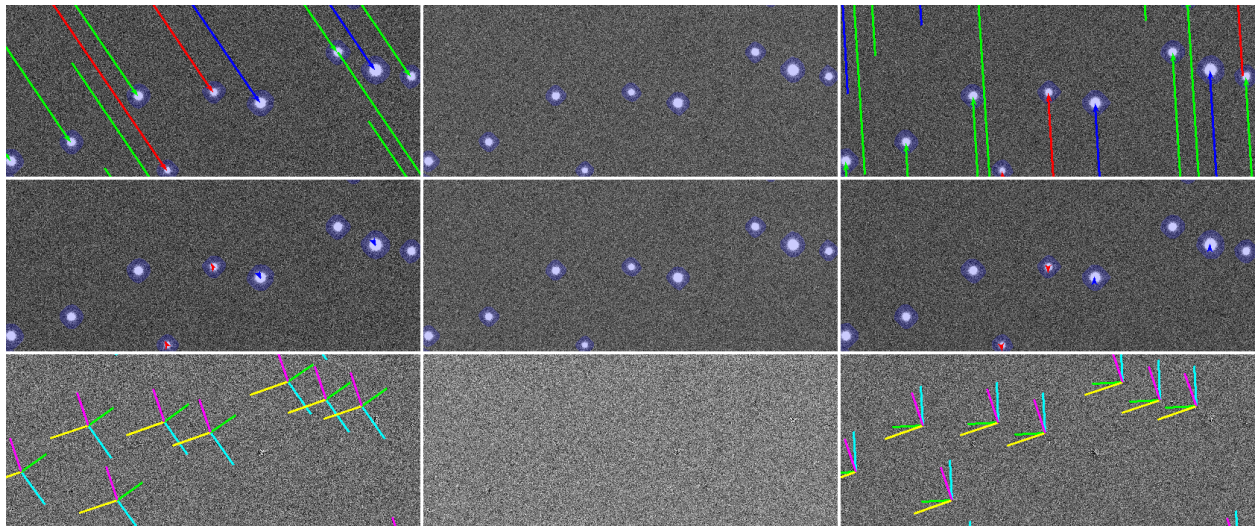


Figure 9: Differential Chromatic Refraction and Difference Image Quality, i -band: Same as Figure 7, but for i -band data. This figure was created using the script `python/compareDcrFromSims.py`.

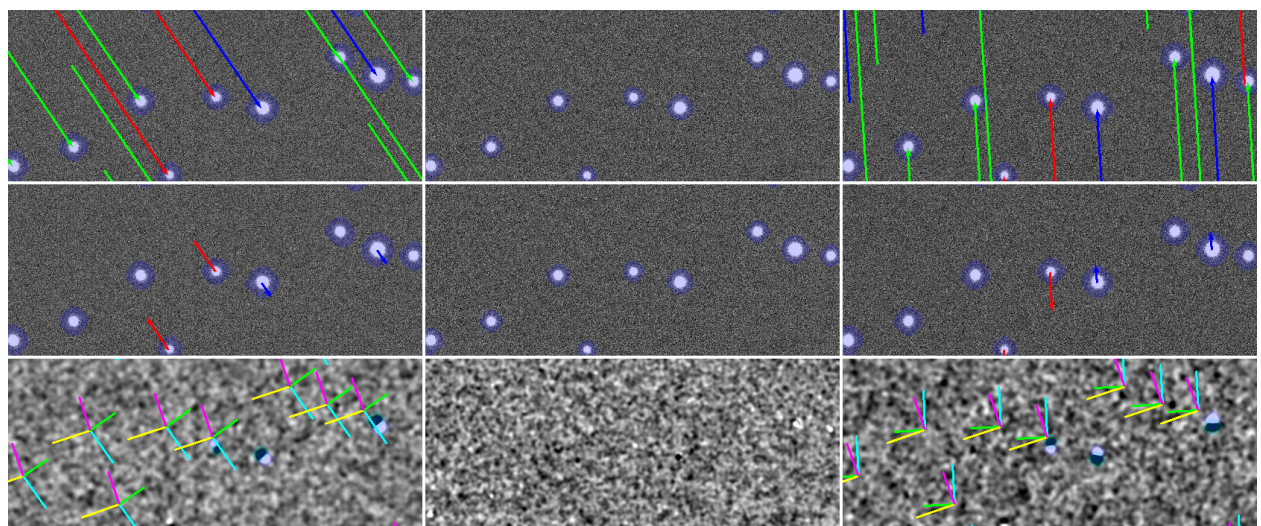


Figure 10: Differential Chromatic Refraction and Difference Image Quality, Prefiltering:
Same as Figure 7, but using prefiltering of the science image with its Psf. This figure was created using the script `python/compareDcrFromSims.py`.

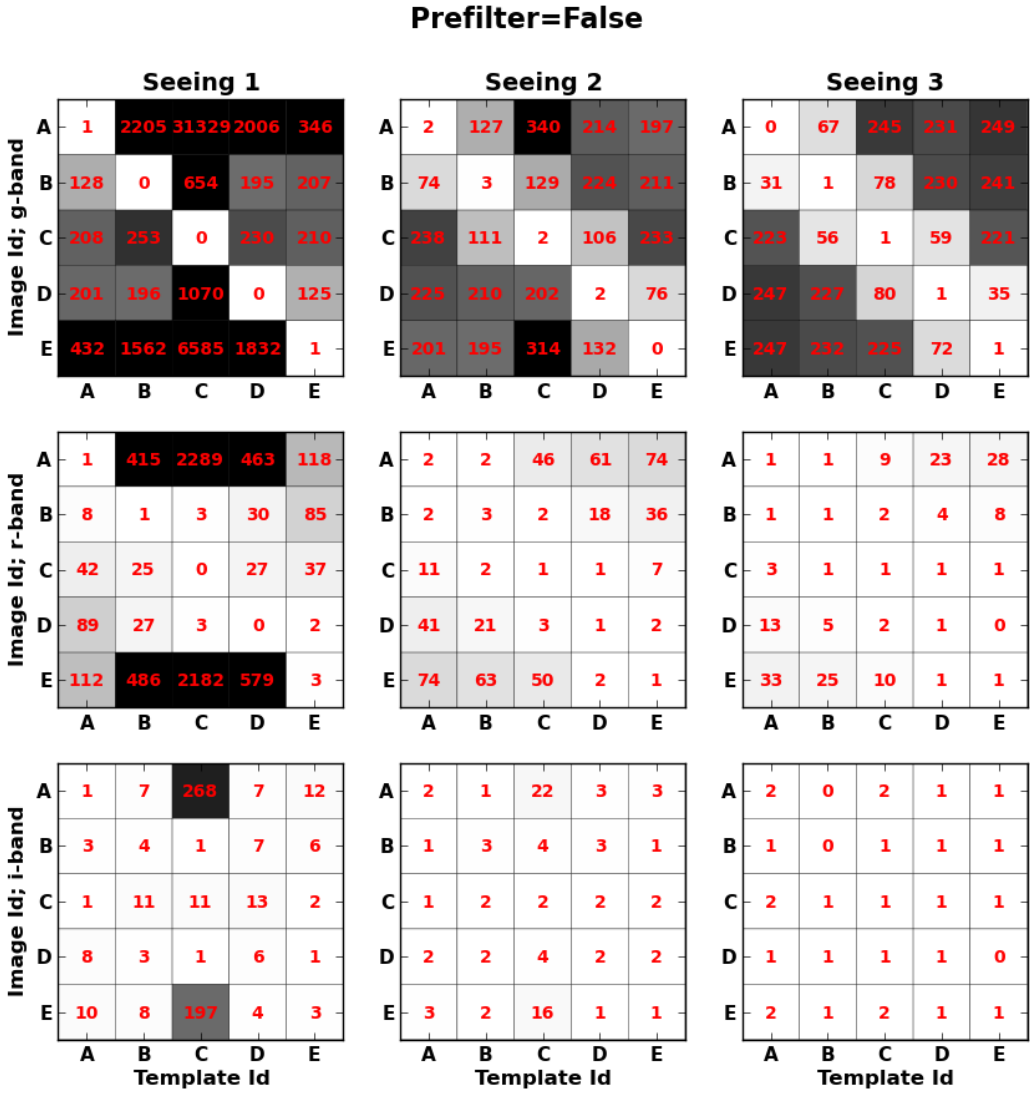


Figure 11: **Number of False Positives, Postfiltering:** This figure shows the median number of false positives across the 9 `raft=2,2` CCDs. The first row of information shows these “heat-maps” for *g*-band data, the second for *r*-band, and the third for *i*-band. The first column represents the good-seeing images, the second the medium-seeing images (same quality as template), and the third the poor-seeing images. Within each filter-seeing combination, the heat-map represents the median number of false positives as a function of the template airmass (visit ABCDE) along the x-axis, and image airmass (visit ABCDE) along the y-axis. The diagonal elements represent the situation where the template and science image are taken at the same airmass and have the same orientation w.r.t. zenith. The off-diagonal elements represent a mismatch between the template and science image in terms of airmass *and* parallactic angle. The general trend is that the numbers of false positives decrease with decreasing differences in the airmass,angle attributes of the template and science image, decrease with increasing seeing, and decrease with increasing wavelength. The *i*-band data in poor seeing do not appear sensitive to Dcr. This figure was created using the script `python/heatMap.py`.

Prefilter=True

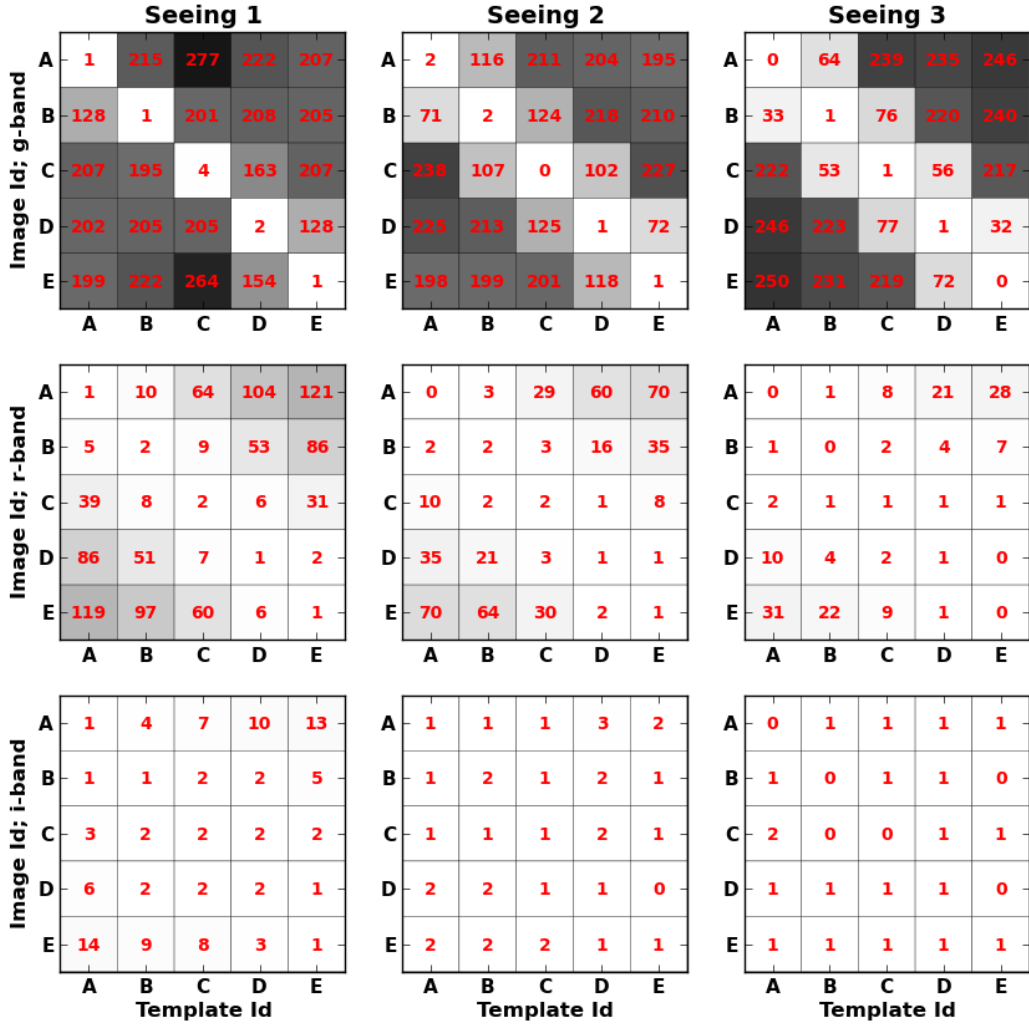


Figure 12: **Number of False Positives, Prefiltering:** Same as Figure 11, but using prefiltering of the science image with its Psf. The numbers of false positives is overall far lower than in the postfiltering case (Figure 11). This figure was created using the script `python/heatMap.py`.

References

Appendices